



Published in final edited form as:

*Sens Actuators A Phys.* 2020 April 15; 305: . doi:10.1016/j.sna.2020.111912.

## Flexible Piezoelectric Nanogenerators Using Metal-doped ZnO-PVDF Films

Congran Jin, Nanjing Hao, Zhe Xu, Ian Trase, Yuan Nie, Lin Dong, Andrew Closson, Zi Chen, John X.J. Zhang\*

Thayer School of Engineering, Dartmouth College, Hanover, NH 03755

### Abstract

Piezoelectric nanomaterial-polymer composites represent a unique paradigm for making flexible energy harvesting and sensing devices with enhanced devices' performance. In this work, we studied various metal doped ZnO nanostructures, fabricated and characterized ZnO nanoparticle-PVDF composite thin film, and demonstrated both enhanced energy generation and motion sensing capabilities. Specifically, a series of flexible piezoelectric nanogenerators (PENGs) were designed based on these piezoelectric composite thin films. The voltage output from cobalt (Co), sodium (Na), silver (Ag), and lithium (Li) doped ZnO-PVDF composite as well as pure ZnO-PVDF samples were individually studied and compared. Under the same experimental conditions, the Li-ZnO based device produces the largest peak-to-peak voltage (3.43 Vpp) which is about 9 times of that of the pure ZnO based device, where Co-ZnO, Na-ZnO and Ag-ZnO are 1.2, 4.9 and 5.4 times, respectively. In addition, the effect of doping ratio of Li-ZnO is studied, and we found that 5% is the best doping ratio in terms of output voltage. Finally, we demonstrated that the energy harvested by the device from finger tapping at ~2 Hz can charge a capacitor with a large output power density of 0.45 W/cm<sup>3</sup> and light up an ultraviolet (UV) light-emitting diode (LED). We also showed the device as a flexible wearable motion sensor, where different hand gestures were detected by the device with distinctive output voltage amplitudes and patterns.

### Graphical abstract

---

\*Corresponding author: Corresponding Author, Professor John X.J. Zhang. john.zhang@dartmouth.edu.

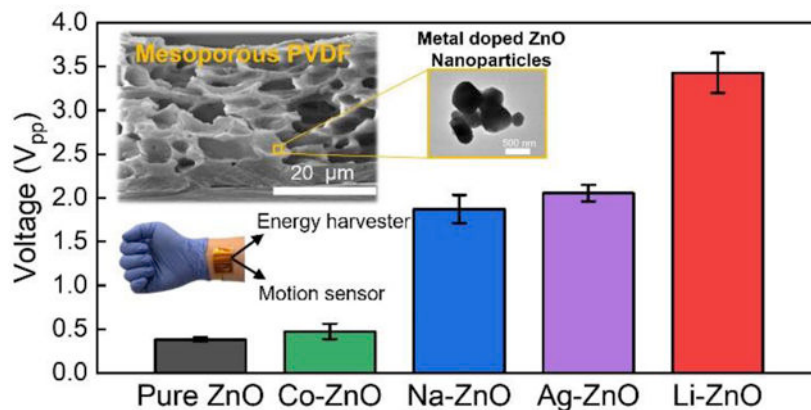
#### Author Contributions

C.J., N.H. Z.X. and X.J.Z conceived the idea of nanomaterials in porous PVDF composite, such as using metal doped ZnO, for compact energy harvesting and sensors designs. C.J. designed and conducted the experiment and wrote the manuscript. N.H. developed the nanoparticle synthesis method and edited the paper. Z.X. developed the experimental setup, conducted the demonstration and edited the manuscript. Y.N. characterized the samples. L.D. and A.C. provided significant discussions and edited the manuscript. Z.C. co-supervised the work. X.J.Z. guided the project, supervised the work and edited the manuscript.

**Publisher's Disclaimer:** This is a PDF file of an unedited manuscript that has been accepted for publication. As a service to our customers we are providing this early version of the manuscript. The manuscript will undergo copyediting, typesetting, and review of the resulting proof before it is published in its final form. Please note that during the production process errors may be discovered which could affect the content, and all legal disclaimers that apply to the journal pertain.

#### CONFLICT OF INTEREST

There are no conflicts to declare.



## Keywords

piezoelectric; ZnO; metal doping; PVDF; flexible energy harvester; sensor

## 1. Introduction

The research for portable and wearable electronics has bloomed in recent years for their diverse applications such as personal communication devices and health monitoring sensors<sup>1</sup>. Powering these electronics in a sustainable and environmental-friendly way has become the goal of the next generation wearable devices. Researchers have developed a variety of small, flexible generators self-powered electronics by converting energy from the ambient or human body motion to electrical energy. One of the emerging technologies is the piezoelectric nanogenerators (PENG), which can convert mechanical strain to electrical energy, for its outstanding energy conversion effectiveness, compactness and simple fabrication. Piezoelectric polymers (such as polyvinylidene fluoride (PVDF) and its copolymer poly(vinylidene fluoride-trifluoroethylene) (P(VDF-TrFE))) are excellent candidates for fabricating wearable and implantable flexible PENG due to the material's flexibility and biocompatibility<sup>1-8</sup>. Zinc oxide (ZnO), that has a hexagonal wurtzite crystalline structure composed of tetrahedrally coordinated  $O^{2-}$  and  $Zn^{2+}$  ions, is another popular material choice for PENG due to its relatively large piezoelectric coefficient ( $d_{33}$ ), abundance, environment-friendly nature and relative biocompatibility.

During the last decade, achieving higher piezoelectric performance for flexible PENG has attracted increasing attention worldwide. Researchers have used various methods to achieve the goal such as introducing ferroelectric effect into PVDF by creating porous structure<sup>9,10</sup> and creating piezoelectric nanocomposites<sup>11,12</sup>. Piezoelectric ceramics (e.g. ZnO) usually have larger  $d_{33}$  values than piezoelectric polymers (e.g. PVDF and its copolymers), but they are too rigid and fragile to be directly used for building flexible devices. Therefore, by incorporating piezoelectric ceramic (e.g. ZnO) into a PVDF matrix, not only is the piezoelectric performance of the composite material significantly improved but its flexibility is also kept<sup>13-22</sup>. In order to further increase the energy output, researchers have doped different metal elements into ZnO nanostructures as the dopant can create defects in the ZnO crystal structure that might improve the piezoelectric performance of ZnO after high voltage

polling<sup>23</sup>. Specifically, when the metal ions are introduced into the ZnO crystal structure, they will occupy the off-center positions and lead to permanent dipoles and ferroelectric effect<sup>24–26</sup>. Researchers have found that the piezoelectric coefficient  $d_{33}$  can be increased by doping iron (Fe)<sup>27</sup>, Cerium (Ce)<sup>24</sup>, gadolinium (Gd)<sup>28</sup>, gallium (Ga)<sup>29</sup>, manganese (Mn)<sup>30</sup>, chromium (Cr)<sup>25</sup>, vanadium (V)<sup>31</sup>, europium (Eu)<sup>26</sup>, cobalt (Co)<sup>32</sup>, or lithium (Li)<sup>33,34</sup> into ZnO nanostructure. However, these findings only focus on the piezoelectric properties (e.g. value of  $d_{33}$ ) of rigid ZnO film specimen doped by an individual metal element without providing information on the actual energy generation (i.e. voltage and power output). Despite the large selection of metal elements in these works, there is still a lack of information on a systematic investigation of metal dopants on power generation performance. This work will endow us a guidance for better material design for flexible PENG in the future. Moreover, although several studies have proposed flexible PENGs made by compositing Co<sup>19</sup>, neodymium (Nd)<sup>35</sup>, yttrium (Y) 36, nickel (Ni) 21, or lithium (Li) 23,37 - doped ZnO with soft polymers such as polydimethylsiloxane (PDMS) and PVDF and reported the power generation of these devices, the key question of how different metal dopants lead to different levels of energy output remain unknown in that each of these devices are tested based on its very unique material system and test condition while a systematic and direct comparison is still missing.

In this work, we developed a small, flexible piezoelectric generator based on metal doped ZnO (mZnO) nanoparticles-porous P(VDF-TrFE) composite with enhanced piezoelectric power generation, and a systematic and direct comparison is carried out to reveal the different energy generation behavior introduced by different metal dopants (i.e. Co, Ag, Na and Li). The mZnO nanoparticles are characterized using transmission electron microscopy (TEM), X-ray powder diffraction (XRD) and energy-dispersive X-ray (EDS) analysis, and the composite film is examined using scanning electron microscopy (SEM). Lastly, we demonstrate the outstanding energy harvesting and sensing capability of the flexible device in response to biomechanical motion. This work not only provides a direct and systematic study on the effect of different metal dopant in increasing the piezoelectric performance of flexible PENG that can serve as a guidance for future material selection, but also introduces a fabrication strategy that can further boost the piezoelectric performance of such flexible energy harvester and motion sensor.

## 2. Experimental

### 2.1 Materials and Reagents

Sodium hydroxide (NaOH), zinc nitrate hexahydrate ( $\text{Zn}(\text{NO}_3)_2 \cdot 6\text{H}_2\text{O}$ ), lithium chloride (LiCl), cobalt chloride ( $\text{CoCl}_2$ ), sodium chloride (NaCl), silver nitrate ( $\text{AgNO}_3$ ) and N,N-Dimethylformamide (DMF) are purchased from Sigma-Aldrich. Poly(vinylidene fluoride-trifluoroethylene) (P(VDF-TrFE)) powder is purchased from Arkema and the polymeric ratio is 70/30 mol.%.

**Metal doped ZnO Nanoparticles Synthesis**—Hydrothermal method is employed to fabricate metal doped ZnO nanoparticles in this work. All reactions occur at room temperature unless otherwise noted. First, 125 mM of NaOH solution and 300 mM of Zn

(NO<sub>3</sub>)<sub>2</sub>•6H<sub>2</sub>O solution are fully mixed together. Then, a doping ratio of 5% of solid powder of LiCl, CoCl<sub>2</sub>, NaCl or silver AgNO<sub>3</sub> are added into the solution followed by 20 minutes of ultrasonication. For LiCl, doping ratio of 1% and 20% are also used for comparison. The doping ratio is defined as the mole ratio of the added metal and Zn. Next, the solution is kept in oven at 100°C for 1 hour for the hydrothermal growth of the crystalline structure of the ZnO. Then, the solution is centrifuged and washed with deionized (DI) water three times and dried. Finally, the dried ZnO sample is annealed at 600°C for 3 hours. For pure ZnO nanoparticle samples, metal salt is not added while all other procedures remain the same.

## 2.2 Device Fabrication.

The energy harvester fabrication process is summarized as the following. First, 15% wt P(VDF-TrFE) solution is prepared by mixing P(VDF-TrFE) powder with DMF with the weight ratio defined by the weight of P(VDF-TrFE) powder divided by the total weight of the solution. Next, a mZnO-P(VDF-TrFE) mixture solution is made by mixing the as-prepared metal doped ZnO nanoparticles with the as-prepared 15% wt P(VDF-TrFE) solution with a mixing ratio of 30% wt (the weight of ZnO ÷ the weight of P(VDF-TrFE) powder). A thin layer (20 nm) of gold electrode is sputtered onto a 50 μm Kapton film with the help of a mask to form the circular or rectangular shape of the gold electrode. Then, the first layer of pure 15% P(VDF-TrFE) solution is spin-coated (1500 RPM, 1 minute) onto the Kapton film with the gold electrode and is dried in an oven at 50°C to form a solid film which prevents probable shorting of the top and bottom electrode. Next, the ZnO - P(VDF-TrFE) mixture solution is spin-coated onto the first solid P(VDF-TrFE) layer (1500 RPM, 1 minute). The sample is immediately transferred into a humidity chamber held (90% relative humidity) for 8 hours. This vapor phase separation method generates the internal porous microstructure inside the ZnO - P(VDF-TrFE) film. Next, the porous P(VDF-TrFE) composite film undergoes an annealing process (135°C, 2 hours) and an electrical poling process in a 50 MV/m electrical field at a 100°C hot plate for an hour. Finally, the top gold electrode of 20 nm thick is sputtered onto the top porous composite film and above the bottom electrode.

## 2.3 Characterization

Transmission electron microscopy (TEM) was performed on a FEI Tecnai F20ST field emission gun (FEG) transmission electron microscope operating at an accelerating voltage of 200 kV. Scanning electron microscopy (SEM) was performed on a FEI Scios2 LoVac dual beam FEG scanning electron microscope operating at 20 kV. The X-ray powder diffraction (XRD) measurement was performed on a Rigaku D/MAX 2000 X-ray diffractometer with Cu-Kα radiation and a scanning speed of 1°/minute. The energy-dispersive X-ray spectroscopic (EDS) measurements were performed with the SDD X-ray detector (Ametek®) attached to the FEI scanning electron microscope.

## 3. Results and Discussions

The key fabrication process of our flexible PENG is depicted in Figure 1A. Before the spin-coating process, we first prepare a 15% wt P(VDF-TrFE) solution without ZnO nanoparticles (dark grey in Figure 1A) and a composite solution (light grey) by mixing a 15% wt P(VDF-TrFE) solution with pure, Co, Na, Ag or Li doped ZnO nanoparticles that are grown

hydrothermally. Then a two-step spin-coating process is carried out to form a layer of pure P(VDF-TrFE) film on a 50  $\mu\text{m}$  thick Kapton film sputtered with gold and then a layer of the composite solution. The bottom layer is to prevent the possible electrical shorting of the device. Before the top composite layer solution dries, the sample is quickly moved to a humidity chamber to create the porous structure. The porous structure greatly increases the compressibility and the charge collecting area in the P(VDF-TrFE), leading to higher energy output<sup>38–40</sup> and can make the film more flexible. Moreover, the pores can introduce ferroelectric effect by creating large change of dipoles moments during compression and releasing of the material, generating enhanced energy output<sup>9,10</sup>. Once the pores are formed, the device is peeled off from glass substrate and undergoes annealing and electrical polling steps to create polarization in both P(VDF-TrFE) and ZnO nanoparticles, and finally another gold electrode is sputtered on the top surface. The cornerstone of our flexible PENG is the two piezoelectric material: P(VDF-TrFE) and ZnO. The piezoelectricity of P(VDF-TrFE) originates from the polarized orientation of the monomer (consisting of hydrogen and fluoride atoms) perpendicular to the polymer chain in its beta phase which is induced by the high voltage polling process<sup>2</sup> (Figure S1). The piezoelectricity of ZnO nanoparticles is owing to the disturbance of the original symmetrical crystalline structure with a neutral overall charge. Specifically, when a strain is applied to the wurtzite structure of ZnO, the crystalline cell becomes asymmetric and induces an electrical dipole which creates an electrical potential difference across the bulk material as a result<sup>41</sup> (Figure S1). Next, we observe the cross-section of the as-prepared film using SEM (Figure 1A). Pores of different sizes are created uniformly across the top composite layer, and ZnO nanoparticles are also present evenly in the same layer (Figure S2). By looking at the ZnO nanoparticles with a much higher magnification using TEM (Figure 1B), we find that, as we expected, they all share similar shapes and sizes regardless of the doped metal or the doping ratio, ruling out the possible effect in the materials piezoelectric performance induced by the shape or size of the ZnO nanoparticles. Figure 1C shows the actual device that is thin ( $\sim 90 \mu\text{m}$ ), flexible and smaller than a U.S. penny.

Before evaluating the metal doping effect on the piezoelectric energy output, we first verify that the metal has been successfully doped into ZnO nanoparticles. XRD is employed to analyze the mZnO nanoparticles (Figure 2). The XRD spectrum for pure, Ag, Li, Co and Na doped ZnO samples are shown in Figure 2A. We only see the (100), (002), (101), (102), (110), (103), (200), (112) and (201) diffraction peaks that corresponds to the wurtzite phase of ZnO (JCPDS file No. 36–1451) for all samples without other diffraction peaks that are usually indications of other possible crystal structures formed by the metals<sup>19,42–44</sup>. In addition, the slight shifting of the diffraction peaks to lower  $2\theta$  angles for all mZnO samples as shown in Figure 2B is attributed to the lattice parameter change in the ZnO crystal structure, probably induced by the substitutional and/or interstitial metal dopants<sup>24,37,45–47</sup>. In addition, EDS analysis is performed to reveal the element content of the ZnO nanoparticles.

Figure 2C–G are the EDS energy spectra of the pure, Ag, Co, Na and Li doped ZnO nanoparticles and they all show the presence of Zn and O. Note that the carbon (C), aluminum (Al), and Ni element are detected from the sample's substrate and holder. Figure 2D and E qualitatively show the presence of the Ag and Co element in the Ag and Co doped

ZnO nanoparticle samples, respectively. The relative low intensity of the metal dopant elements in the EDS spectra is due to their extremely small amount. The only characteristic energy of Na ( $K\alpha$ ) is 1.0721 KeV which is very close to the Zn's  $L\alpha$  energy (1.012 KeV), and consequently the peak for Na is completely overlapped by that of Zn and cannot be observed in Figure 2F. Also, since Li has a very low characteristic radiation energy, it cannot be detected by our X-ray detector (Figure 2G) without a major modification to the EDS detector<sup>48</sup>. However, the atomic ratio of Zn:O in pure, Na and Li doped ZnO nanoparticles are 1, 0.83 and 0.72, respectively, indicating the deficiency of Zn atoms in the Na and Li doped ZnO samples, which is possibly owing to the Na/Li dopants substituting Zn atoms, the hydroxyl groups and absorbed H<sub>2</sub>O in the sample<sup>49</sup>. Therefore, provided the crystalline analysis of XRD and element analysis of EDS spectrum for all samples, we may safely assume that the metals have been successfully doped into the ZnO crystal structure.

Next, we evaluate the piezoelectric performance of our mZnO-P(VDF-TrFE) composite based flexible energy harvester and compare various dopants' influence on the voltage output. To do so, we carefully designed a striking test platform (schematic shown in the inset of Figure 3a) that include a vertical wall to which the device is mounted, a shaker (Model 2060E, The Modal Shop) and a force transducer (Model 208C02PCB Piezotronics). The shaker applies a force of 0.8 N at 1 Hz perpendicular to the surface of the device (active area: 0.8 cm<sup>2</sup>) and the output voltage is measured using an oscilloscope (TDS 2014B, Tektronix). Examples of the raw open-circuit voltage for different metal doped devices are shown in Figure 3A. The positive and negative voltage responses correspond to the compression and recovery status of the composite film, respectively (Figure 3A). The average peak-to-peak voltages ( $V_{pp}$ ) are shown in Figure 3B. It is found that the voltage of the Co-ZnO device ( $\sim 0.47 V_{pp}$ ) is only slightly higher than that of the pure ZnO device ( $\sim 0.38 V_{pp}$ ), while the voltage of Na and Ag-ZnO devices ( $\sim 1.87 V_{pp}$  and  $\sim 2.04 V_{pp}$ , respectively) is about 5 times as large as that of the pure ZnO devices. The most significant increase of voltage output comes from Li-ZnO device which generates a 3.43  $V_{pp}$  which is about 9 times as large as the pure ZnO device. The significant enhancement of piezoelectric voltage output of the Li-ZnO based device is owing to the electric polarization in the ZnO nanoparticles after high voltage polling<sup>23</sup>. To study the effect of dopant ratio, we fabricated two other Li-ZnO devices with 1% and 20% doping ratio (see Experiments for details) to compare with the previously test 5% Li-ZnO device. With all test conditions kept the same, the voltage output of 1%, 5% and 20% Li based device are 0.58  $V_{pp}$ , 3.43  $V_{pp}$  and 2.09  $V_{pp}$ , respectively (Figure, 3C and 3D). All three concentrations increase the voltage output from that of the pure ZnO based device (0.38  $V_{pp}$ ). However, as the Li concentration increases from 5% to 20%, the voltage output drops, suggesting that over-doping metal ions into ZnO nanostructure plays a counterproductive role in the energy generation process, which is in a good agreement with previous findings<sup>23,31</sup>. When the dopant concentration initially increases, the substitutional and interstitial defects introduced by the dopants breaks the original symmetry of the ZnO wurtzite structure, thereby creating an electrical dipole that enhances piezoelectricity. Nevertheless, as the doping concentration further increases, excessive defects and free charge carriers in the ZnO nanostructure induces a piezoelectric potential screening effect that undermines the material's piezoelectricity<sup>23,50</sup>. In addition, excessive dopants also lead to crystallite disorientation and amorphization of ZnO<sup>45</sup> that can

substantially weaken the piezoelectric performance of the material<sup>31</sup>. Furthermore, we have measured the dielectric constant for the Li-ZnO and pure ZnO device, and it is found that the Li doping has increased the dielectric constant in the AC frequency range of 0.1 – 10 kHz (Figure S3).

Lastly, we demonstrate our flexible energy generator's potential in powering small electronics using collected biomechanical energy and showcase its sensing capabilities from human hand and wrist motion. With material synthesis and device fabrication processes kept the same for consistency, an enlarged version ( $4 \times 3$  cm) of the device is fabricated to further amplify the power output of our device using 5% Li-ZnO nanoparticles for its superior energy performance. The electric circuit we use to carry the test is shown in Figure 4A, in which our energy harvester directly powers a UV LED through a preamplifier or charges a capacitor through a rectifier that converts the input AC voltage to DC voltage. As shown in Figure 4B and SI Movie 1, by gently tapping the device using one or two fingers, the UV LED that requires a 3.2 V voltage input is lit up. Next, we use similar finger tapping motion to charge a 150  $\mu$ F capacitor at a tapping frequency of  $\sim 2$  Hz (Figure 4C). The stepwise voltage increase during the charging process can be clearly seen from the voltage vs. time curve, and each increment corresponds to a tapping action. The power (P) generated from this biomechanical energy is calculated to be 53.4  $\mu$ W using the equation  $P = \frac{CV^2}{2t}$ , where  $C$ ,  $V$  and  $t$  is the capacitance (F), voltage (V) and time (s), respectively, and the corresponding energy density is 0.494 W/cm<sup>3</sup> for our device.

This device can also be used as a sensor to monitor human body motion in real time. As a demonstration, we mount the flexible device onto the ventral side of a volunteer's wrist (Figure 4D) and ask the volunteer to perform three different hand actions, namely hand grasping, wrist twisting and fist squeezing in a cyclic manner while monitoring the voltage output from an oscilloscope (Figure 4E; SI Movie 2, 3 and 4). Each voltage curve induced by these movement is distinguishable in terms of the signal's amplitude and curve pattern. For example, the grasping motion creates the largest voltage amplitude ( $\sim 100$  mV) as this motion is most dramatic that induces greater extension and contraction of the muscles in the wrist such as the flexor carpi radialis tendon, the flexor digitorum superficialis tendons and the palmaris longus tendon. On the other hand, the twisting and squeezing motion involve smaller-scale muscle movement, so their voltage amplitudes are as low as 20 – 40 mV. Also, we notice that the output voltage pattern generated by twisting is especially distinct from those of the other two as it has more peaks in a voltage period. This is likely due to the more complex deformation of the film induced by the twisting movement of the muscles.

Admittedly, in the ZnO nanoparticles synthesis process, the Na<sup>+</sup> in the NaOH solution may not be reacted completely and leave some residual Na<sup>+</sup> ions that might be active in the later metal doping step. However, the effect is trivial to our study for two reasons. First, only a small amount (compared to the later doped metals), if any, of Na<sup>+</sup> is left without being fully reacted. Second, all ZnO nanoparticle samples, including pure ZnO and mZnO, are fabricated strictly using the same procedure under the same condition, hence providing a consistent baseline for the comparison study in this work.

Several hypotheses have been proposed to describe how different dopants can tune the piezoelectric performance of ZnO by correlating the dopant ionic size with the piezoelectric coefficient of ZnO. Luo et al.<sup>27</sup> state that the  $d_{33}$  value of ZnO will be increased if the size of dopant transition metal ion is smaller than that of  $Zn^{2+}$  and will be decreased if the dopant is larger. Zhang et al.<sup>51</sup> ascribe the enhancement of the output voltage of ZnO-based PENG to the increasing lattice strain created by the doped halogen elements. More recently, Sinha and coworkers<sup>36</sup> find that the value of  $d_{33}$  is correlated to the ratio  $\left(\frac{\text{ionic charge}}{\text{crystal radius}}\right)$  of the metal dopant and show that the larger the ratio, the higher the  $d_{33}$  value in general. All these hypotheses are based on limited selection of dopants and heavily rely on their ionic or crystal radii. Nevertheless, the actual properties such as ionic or crystal radius and the charge status of the metal dopants in the ZnO nanostructure is very complicated and may be heterogeneous<sup>52</sup>. For that reason, future research is needed to carefully study the fundamental mechanism of the doping effect, including accurately identifying the actual ionic radius of the dopant, on the piezoelectric performance of ZnO. This work focuses on providing a systematic and a direct comparison of the doping effect in the context of a flexible energy generator built on ZnO nanoparticle-PVDF composite. There is still a long road ahead for powering electronic devices using sustainable energy such as human body motion that will be otherwise wasted. Fortunately, with countless efforts made during the last decade, we finally had clues on how to select and design the material so that it can optimize the energy conversion performance.

#### 4. Conclusion

In this work, we have developed a metal ZnO nanoparticle-P(VDF-TrFE) composite based flexible piezoelectric energy generator with enhanced piezoelectric performance. We systematically characterized the performance of pure, Co, Na, Ag and Li doped ZnO devices. We identified that the 5% Li doped device, which has increased the voltage output to 9 times than a pure ZnO device, is the best among all metal dopant device in terms of voltage generation. Moreover, we demonstrated that the device is a promising prototype for powering small electronics by harvesting biomechanical energy and detecting human body motions as a flexible wearable motion sensor. This work reveals the different effects of the metal dopant on the piezoelectric performance of flexible PENG which can serve as a guidance for future material selection and introduces a designing strategy to improve piezoelectric performance of such flexible energy harvester and motion sensor.

#### Supplementary Material

Refer to Web version on PubMed Central for supplementary material.

#### ACKNOWLEDGMENT

The authors acknowledge financial support from the National Institute of Health (NIH) Director's Transformative Research Award (R01HL137157, PI: X.J.Z.), the National Science Foundation award (ECCS1509369, PI: X.J.Z.), and the startup fund from the Thayer School of Engineering at Dartmouth. Z.C. also acknowledges support from the Branco Weiss-Society in Science fellowship, administered by ETH Zürich. C.J. is thankful for the discussion and help of characterization from Dr. Maxime Guinel in the EM facility as well as Cory T Cline, Sidan Fu, Yiwen Zhang, Chuanlong Wang and Can Xu in the Thayer School of Engineering at Dartmouth College.



#### Funding Sources

National Institute of Health (NIH) Director's Transformative Research Award (R01HL137157, PI: X.J.Z.). The National Science Foundation award (ECCS1509369, PI: X.J.Z.). The startup fund from the Thayer School of Engineering at Dartmouth.

## Biographies

### Congran Jin:

Mr. Jin is currently a Ph.D candidate at Thayer School of Engineering at Dartmouth College, Hanover, NH, USA. He obtained his B.S. and M.S. degree in Mechanical Engineering from Rensselaer Polytechnic Institute (RPI), Troy, NY in 2016. His research interest includes piezoelectric energy harvesters, sensors, functional nanoparticle synthesis and soft robots.

### Nanjing Hao:

Dr. Nanjing Hao is a research associate at the Thayer School of Engineering, Dartmouth College (currently working at Duke University). He obtained his bachelor's degree of bioengineering (2009) and PhD degree of chemistry (2014) in P.R. China. His current research interest is focusing on microfluidics-enabled on-chip colloidal materials synthesis for applications in liquid biopsy, biosensor, catalysis, and environment.

### Zhe Xu:

Dr. Zhe Xu received his M.S. (2014) degree and Ph.D. (2017) degree from Erik Jonsson School of Engineering and Computer Science at University of Texas at Dallas, Dallas, Texas. Currently he is a research associate of Professor John X.J. Zhang's lab in Thayer school of Engineering at Dartmouth College, Hanover, New Hampshire. His research interest lies at piezoelectric composite materials, bio-inspired materials, advanced manufacturing, implantable energy harvesting application, and bio-integration of soft electronics.

### Ian Trase:

Ian Trase received his Bachelor's degree in Mechanical Engineering from Princeton University in 2014 with certificates in Materials Science and Engineering Physics. Ian's research experiences include internships at the Princeton Electric Propulsion Laboratory and MIT CSAIL. He is currently a Ph.D. Innovation Fellow at the Thayer School of Engineering at Dartmouth, where his research focuses on flexible electronics and wearable haptics with an interest in translating technologies out of the lab to commercial applications.

### Yuan Nie:

Yuan Nie received her BS degree (2011) and MS degree (2014) in Mechanical Engineering in P.R. China. She is currently a Ph.D. candidate at Thayer School of Engineering, Dartmouth College, NH, USA. Her research interests are the development of microfluidic reactors, synthesis of nanomaterials, on-chip biosensing and cell analysis.

Lin Dong:

Dr. Dong is a Research Associate at Thayer School of Engineering at Dartmouth College. She obtained her Ph.D. from the Department of Mechanical Engineering at Stevens Institute of Technology, where she was awarded an Innovation and Entrepreneurship Doctoral Fellowship. Her research interests include advanced materials for implantable and wearable energy devices and actuating and sensing devices using soft materials.

Andrew Closson

Andrew Closson is a Ph.D. candidate under the supervision of Professor John X.J. Zhang at Thayer School of Engineering at Dartmouth College. He received his B.Sc. degree in Bioengineering from the University of Maine in 2016. His research focuses on the development of materials and devices for energy harvesting applications in biomedical devices.

Zi Chen:

Dr. Zi Chen is currently a tenure-track Assistant Professor at Thayer School of Engineering and an adjunct Assistant Professor in Department of Biological Sciences at Dartmouth College, Hanover, NH, USA. Dr. Chen received his PhD in Mechanical and Aerospace Engineering at Princeton University in 2012. His research interests range from solid mechanics and material science to biomechanics and mechanobiology. He has received a number of awards and honors including Society in Science – Branco Weiss fellowship, Marquis Who's Who in the World, Outstanding Paper Award at the ASME 2013 2nd Global Congress on NanoEngineering for Medicine and Biology (NEMB), American Academy of Mechanics Founder's Award, etc.

John X.J. Zhang:

Dr. Zhang is a Professor at the Thayer School of Engineering, Dartmouth College, NH, USA, and a Fellow of AIMBE. He received his PhD from Stanford University, CA, USA. His research is on developing miniature medical systems to improve global health, through innovations in bio-inspired nanomaterials, lab-on-chip design, and advanced nanofabrication technologies. He is a recipient of numerous prestigious awards, including NSF Career award, DARPA Young Faculty Award, Wallace Coulter Foundation Early Career Award and NIH Director's Transformative Research Award. Dr. Zhang has mentored over 30 Ph.D. students and post-doctoral scholars, and published a textbook in biomedical engineering.

## REFERENCES

1. Fan FR, Tang W and Wang ZL, *Adv. Mater.*, 2016, 28, 4283–4305. [PubMed: 26748684]
2. Chorsi MT, Curry EJ, Chorsi HT, Das R, Baroody J, Purohit PK, Ilies H and Nguyen TD, *Adv. Mater.*, 2018, 31, 1–15.
3. Dong L, Han X, Xu Z, Closson AB, Liu Y, Wen C, Liu X, Escobar GP, Oglesby M, Feldman M, Chen Z and Zhang JXJ, *Adv. Mater. Technol.*, 2019, 4, 1–9.
4. Dong L, Wen C, Liu Y, Xu Z, Closson AB, Han X, Escobar GP, Oglesby M, Feldman M, Chen Z and Zhang JXJ, *Adv. Mater. Technol.*, 2019, 4, 1–9.

5. Xu Z, Liu Y, Dong L, Closson AB, Hao N, Oglesby M, Escobar GP, Fu S, Han X, Wen C, Liu J, Feldman MD, Chen Z and Zhang JXJ, *ACS Appl. Mater. Interfaces*, 2018, 10, 33516–33522. [PubMed: 30199624]
6. Won SS, Sheldon M, Mostovych N, Kwak J, Chang BS, Ahn CW, Kingon AI, Kim IW and Kim SH, *Appl. Phys. Lett*, 2015, 107, 202901.
7. Fan FR, Tian ZQ and Lin Wang Z, *Nano Energy*, 2012, 1, 328–334.
8. Dong L, Closson AB, Jin C, Trase I, Chen Z and Zhang JXJ, *Adv. Mater. Technol*, 2019, 1900177, 1–28.
9. Li W, Torres D, Díaz R, Wang Z, Wu C, Wang C, Lin Wang Z and Sepúlveda N, *Nat. Commun*, 2017, 8, 15310.
10. Li W, Torres D, Wang T, Wang C and Sepúlveda N, *Nano Energy*, 2016, 30, 649–657.
11. Zhang Y, Zhu W, Jeong CK, Sun H, Yang G, Chen W and Wang Q, *RSC Adv*, 2017, 7, 32502–32507.
12. Moorthy B, Baek C, Wang JE, Jeong CK, Moon S, Il Park K and Kim DK, *RSC Adv*, 2017, 7, 260–265.
13. Sorayani Bafqi MS, Bagherzadeh R and Latifi M, *J. Polym. Res*, 2015, 22, 1–9.
14. Kang HB, Han CS, Pyun JC, Ryu WH, Kang CY and Cho YS, *Compos. Sci. Technol*, 2015, 111, 1–8.
15. Nunes-Pereira J, Sencadas V, Correia V, Rocha JG and Lanceros-Méndez S, *Sensors Actuators, A Phys*, 2013, 196, 55–62.
16. Zeng W, Tao XM, Chen S, Shang S, Chan HLW and Choy SH, *Energy Environ. Sci*, 2013, 6, 2631–2638.
17. Chang J, Dommer M, Chang C and Lin L, *Nano Energy*, 2012, 1, 356–371.
18. Lee M, Chen CY, Wang S, Cha SN, Park YJ, Kim JM, Chou LJ and Wang ZL, *Adv. Mater*, 2012, 24, 1759–1764. [PubMed: 22396355]
19. Parangusan H, Ponnamma D and Al-Maadeed MAA, *Sci. Rep*, 2018, 8, 1–11. [PubMed: 29311619]
20. Li J, Chen S, Liu W, Fu R, Tu S, Zhao Y, Dong L, Yan B and Gu Y, *J. Phys. Chem. C*, 2019, 123, 11378–11387.
21. Parangusan H, Ponnamma D and Al Ali Almaadeed M, *RSC Adv*, 2017, 7, 50156–50165.
22. Hao N, Xu Z, Nie Y, Jin C, Closson AB, Zhang M and Zhang JXJ, *Chem. Eng. J*, 2019, 378, 122222. [PubMed: 32831625]
23. Shin SH, Kim YH, Lee MH, Jung JY, Seol JH and Nah J, *ACS Nano*, 2014, 8, 10844–10850. [PubMed: 25265473]
24. Sinha N, Ray G, Bhandari S, Godara S and Kumar B, *Ceram. Int*, 2014, 40, 12337–12342.
25. Kumar B, Sinha N, Ray G, Godara S and Gupta MK, *Mater. Res. Bull*, 2014, 59, 267–271.
26. Yadav H, Sinha N, Goel S and Kumar B, *J. Alloys Compd*, 2016, 689, 333–341.
27. Luo JT, Yang YC, Zhu XY, Chen G, Zeng F and Pan F, *Phys. Rev. B - Condens. Matter Mater. Phys*, 2010, 82, 1–7.
28. Goel S, Sinha N, Yadav H, Godara S, Joseph AJ and Kumar B, *Mater. Chem. Phys*, 2017, 202, 56–64.
29. Zhao T, Fu Y, Zhao Y, Xing L and Xue X, *J. Alloys Compd*, 2015, 648, 571–576.
30. Vladut CM, Mihaiu S, Tenea E, Preda S, Calderon-Moreno JM, Anastasescu M, Stroescu H, Atkinson I, Gartner M, Moldovan C and Zaharescu M, *J. Nanomater*, 2019, 2019, 1–12.
31. Laurenti M, Castellino M, Perrone D, Asvarov A, Canavese G and Chiolerio A, *Sci. Rep*, 2017, 7, 1–13. [PubMed: 28127051]
32. D’Agostino D, Di Giorgio C, Di Trollo A, Guarino A, Cucolo AM, Vecchione A and Bobba F, *AIP Adv*, 2017, 7, 055010.
33. Zhao X, Li S, Ai C, Liu H and Wen D, *Micromachines*, 2019, 10, 212.
34. Wang XS, Wu ZC, Webb JF, Liu ZG, Bundesmann C, Ashkenov N, Schubert M, Spemann D, Butz T, Kaidashev EM, Lorenz M, Grundmann M, Shin SH, Kim YH, Lee MH, Jung JY, Seol JH, Nah

- J, Zeng YJ, Ye ZZ, Xu WZ, Li DY, Lu JG, Zhu LP, Zhao BH, Chang YT, Chen JY, Yang TP, Huang CW, Chiu CH, Yeh PH and Wu WW, *Appl. Phys. Lett*, 2003, 8, 291–296.
35. Batra K, Sinha N, Goel S, Yadav H, Joseph AJ and Kumar B, *J. Alloys Compd*, 2018, 767, 1003–1011.
36. Sinha N, Goel S, Joseph AJ, Yadav H, Batra K, Gupta MK and Kumar B, *Ceram. Int*, 2018, 44, 8582–8590.
37. Chowdhury AR, Abdullah AM, Hussain I, Lopez J, Cantu D, Gupta SK, Mao Y, Danti S and Uddin MJ, *Nano Energy*, 2019, 61, 327–336.
38. Chen D, Sharma T and Zhang JXJ, *Sensors Actuators, A Phys*, 2014, 216, 196–201.
39. Chen D, Chen K, Brown K, Hang A and Zhang JXJ, *Appl. Phys. Lett*, 2017, 110, 0–5.
40. Yu Y, Sun H, Orbay H, Chen F, England CG, Cai W and Wang X, *Nano Energy*, 2016, 27, 275–281. [PubMed: 28626624]
41. Wang ZL, *Mater. Sci. Eng. R Reports*, 2009, 64, 33–71.
42. Sánchez Zeferino R, Barboza Flores M and Pal U, *J. Appl. Phys*, 2011, 109, 014308.
43. Rahmati A, Balouch Sirgani A, Molaei M and Karimipour M, *Eur. Phys. J. Plus*, 2014, 129, 250.
44. Tabib A, Bouslama W, Sieber B, Addad A, Elhouichet H, Férid M and Boukherroub R, *Appl. Surf. Sci*, 2017, 396, 1528–1538.
45. Nakrela A, Benramdane N, Bouzidi A, Kebbab Z, Medles M and Mathieu C, *Results Phys*, 2016, 6, 133–138.
46. Rajesh Kumar B and Hymavathi B, *J. Asian Ceram. Soc*, 2017, 5, 94–103.
47. Ginting M, Taslima S, Sebayang K, Aryanto D, Sudiro T and Sebayang P, in *AIP Conference Proceedings*, 2017, vol. 1862.
48. Hovington P, Timoshevskii V, Burgess S, Demers H, Statham P, Gauvin R and Zaghbi K, *Scanning*, 2016, 38, 571–578. [PubMed: 26840888]
49. Kim KJ, Kreider PB, Choi C, Chang CH and Ahn HG, *RSC Adv*, 2013, 3, 12702–12710.
50. Romano G, Mantini G, Di Carlo A, D'Amico A, Falconi C and Wang ZL, *Nanotechnology*, 2011, 22, 465401. [PubMed: 22024724]
51. Zhang Y, Liu C, Liu J, Xiong J, Liu J, Zhang K, Liu Y, Peng M, Yu A, Zhang A, Zhang Y, Wang Z, Zhai J and Wang ZL, *ACS Appl. Mater. Interfaces*, 2016, 8, 1381–1387. [PubMed: 26704902]
52. Shannon RD, *Acta Crystallogr*, 1976, A32, 751.

**Highlights:**

- Co, Na, Ag and Li ions are doped into ZnO for piezoelectric performance improvement.
- Li-ZnO device produces voltage of 3.43 V which is 9 times of pure ZnO device.
- Flexible nanogenerators are built by PVDF and metal doped ZnO nanoparticles.
- The flexible energy harvester generates 53.4  $\mu$ W power with finger movements.
- The wearable sensors can detect different modes of wrist and hand gestures.

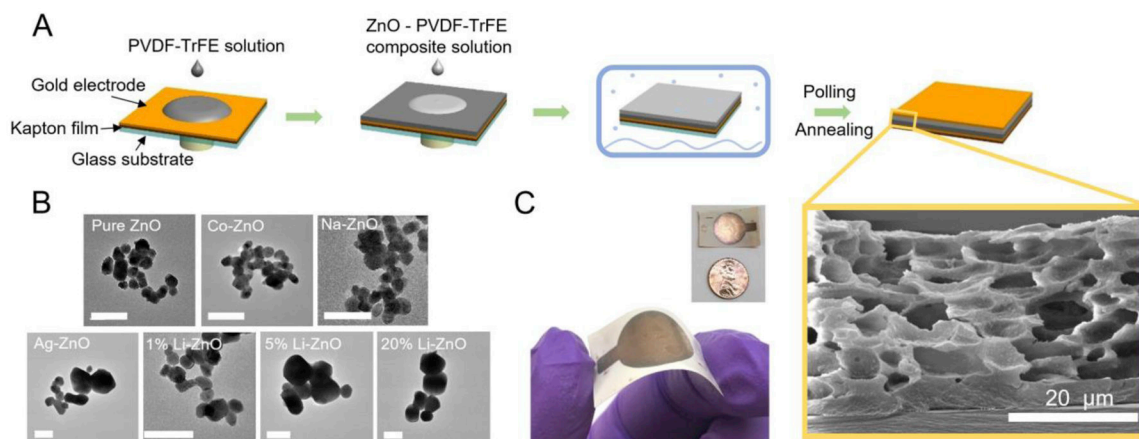


**Figure 1.**

Overview of the metal doped ZnO (mZnO) nanoparticle-P(VDF-TrFE) Composite device.

A. Schematic of the key fabrication process of the device including a SEM image of the cross section of the device showing the porous structure of the P(VDF-TrFE) film mixed ZnO nanoparticles (Figure S2). B. TEM image of pure, Co, Na, Ag and 1, 5, 20% Li doped ZnO nanoparticles. The scale bar is 500 nm. C. The thin film based flexible energy harvester and sensor prototype with a U.S. penny coin for scale.

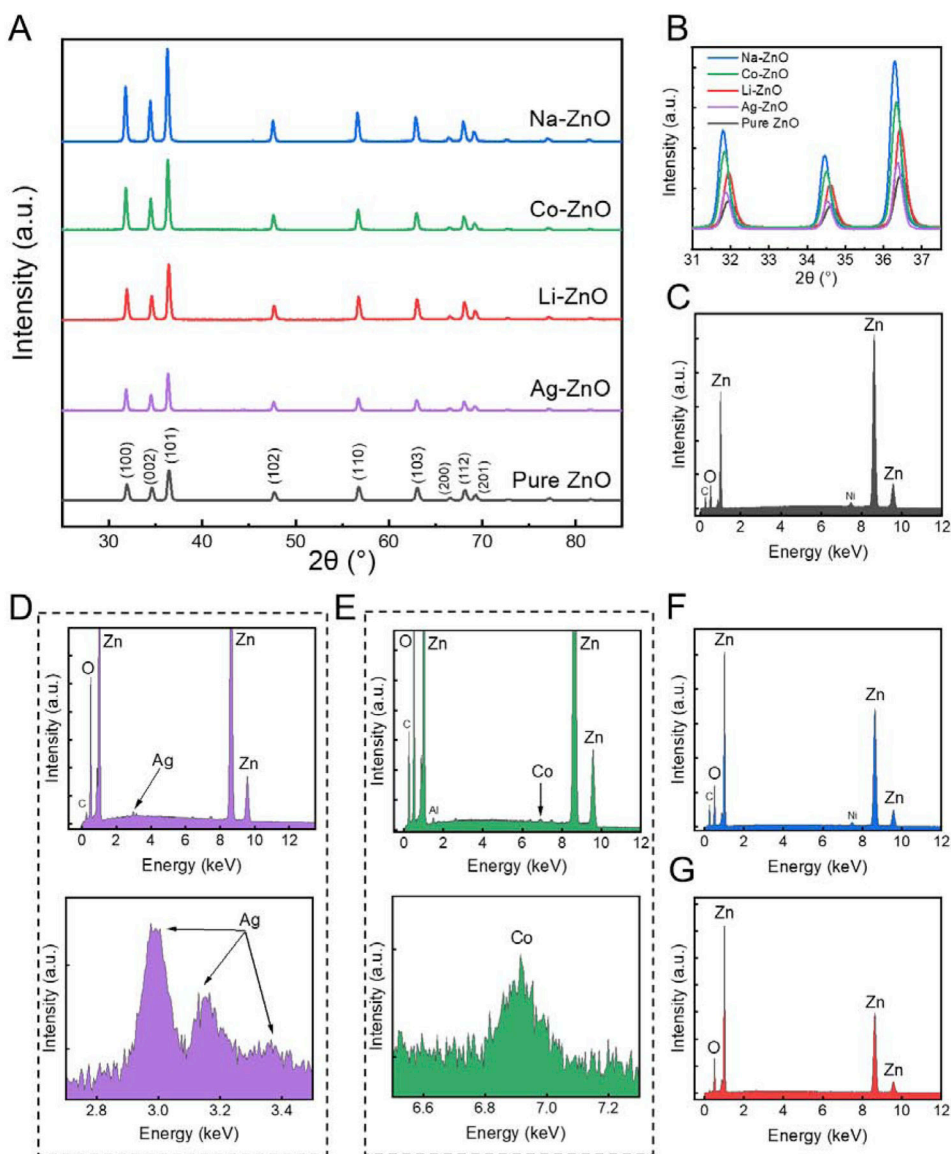


**Figure 2.** Characterization of the metal doped ZnO nanoparticles. A. XRD spectrum of pure, Na, Co, Li and Ag doped ZnO nanoparticles showing only characteristic ZnO peaks without peaks of the metal dopant. B. Shift of peaks observed from the mZnO nanoparticles indicating the doping of the metal ions. C. The EDS energy spectrum of the pure ZnO, D. Ag doped ZnO, E. Co doped ZnO, F. Na doped ZnO, and G. Li doped ZnO nanoparticles.

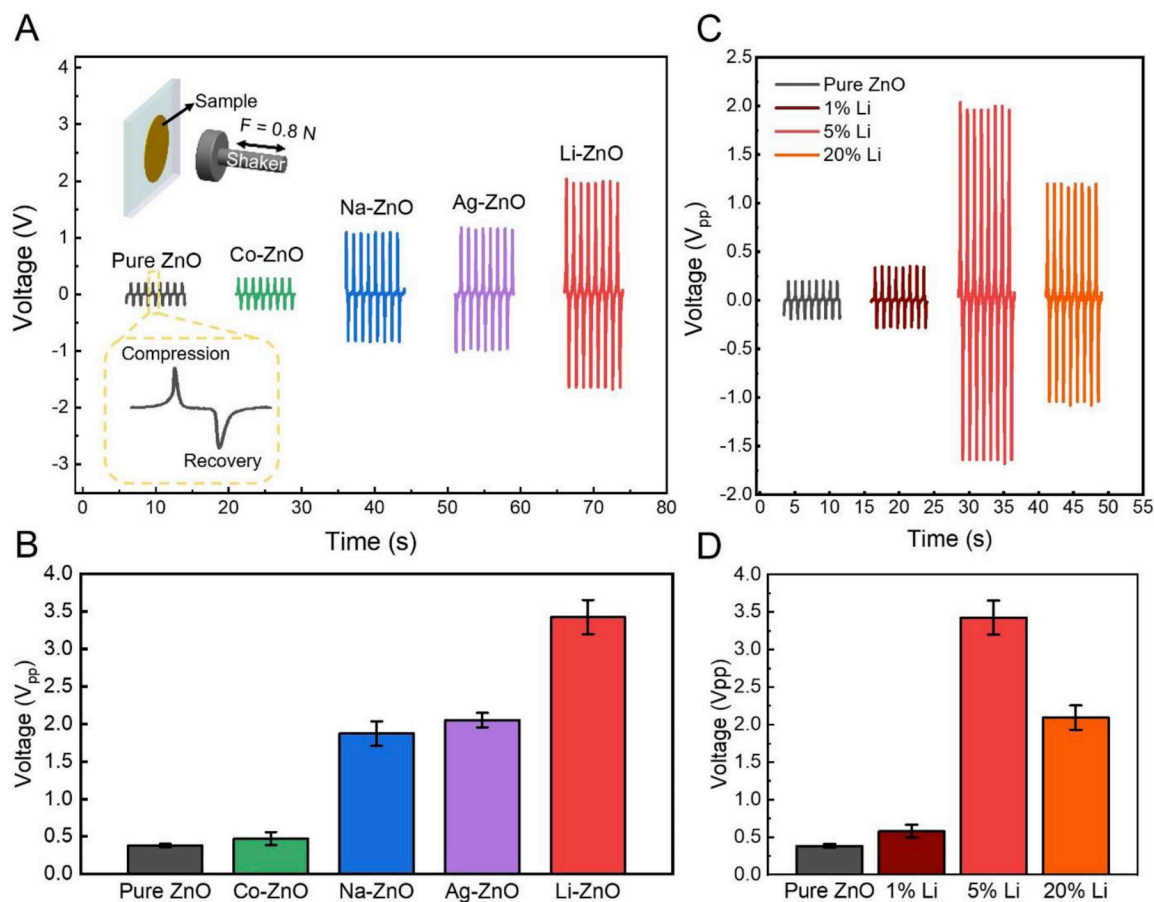


**Figure 3.**

The energy output performance different metal doped ZnO nanoparticle-based devices. A. The raw voltage output from pure, Co, Na, Ag and Li-ZnO nanoparticle-based devices. The inset is the test setup with an impact force of 0.8 N. B. The average voltage output from all devices in A. C. The raw voltage output from the 1, 5 and 20% Li-ZnO nanoparticle-based devices. D. The average voltage output for all devices in C. The error bar is standard deviation of triple measurements.



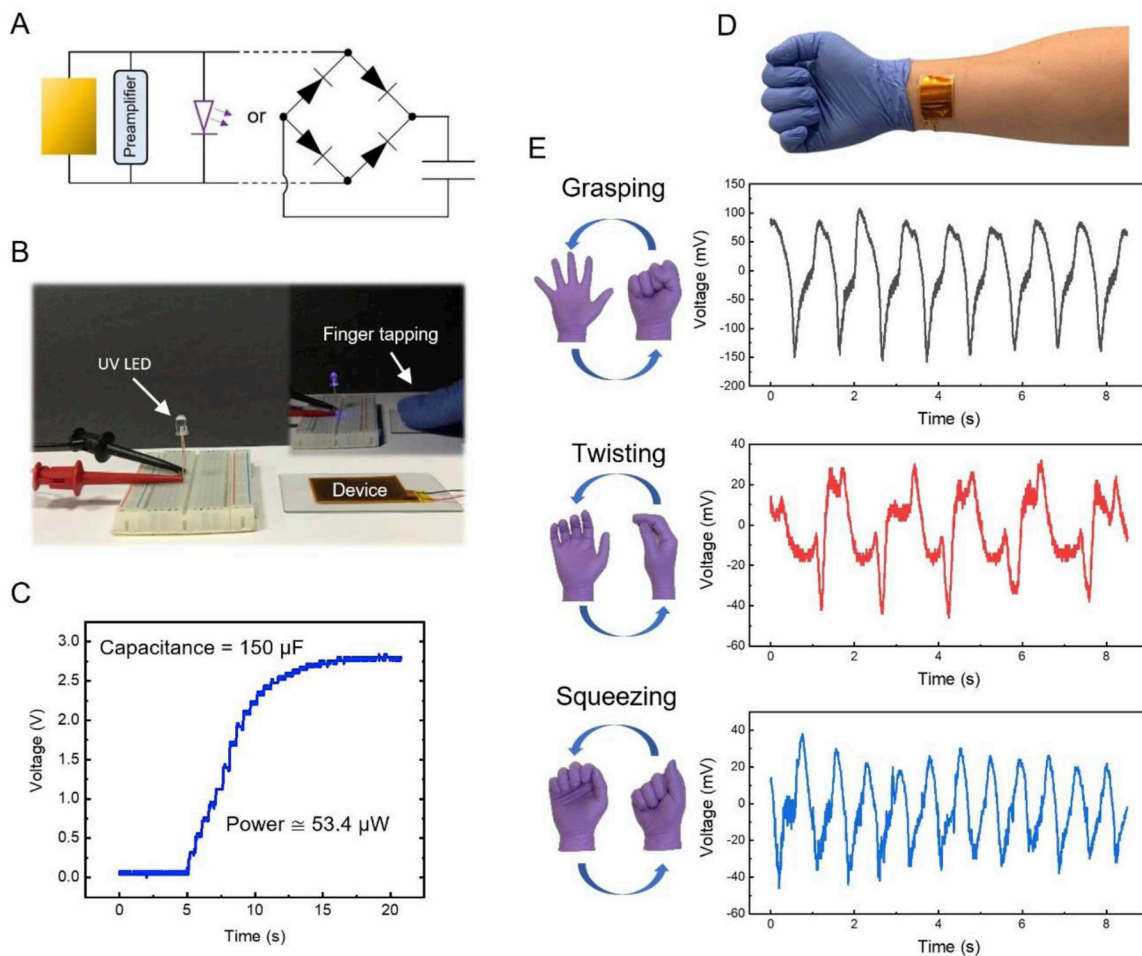


**Figure 4.** Demonstration of the device as a compact energy harvester and a wearable hand motion sensor. A. The electric circuit schematic for energy harvesting test. B. Picture of the energy harvesting test setup in which a finger tapping the device lights up a UV LED (the inset picture). C. The voltage vs. time curve of a 150  $\mu$ F capacitor being charged by tapping the device using a finger with a power generation of  $\sim$  53.4  $\mu$ W. D. Picture of the flexible device as a motion sensor attached to the ventral side of the wrist. E. Different hand/wrist motions detected by the device in the form of voltage output with distinctive amplitudes and patterns.